

Minimization of DC Reactor and Operation Characteristics of Direct-Power-Controlled Current-Source PWM Rectifier

Toshihiko Noguchi, Akira Sato, and Daisuke Takeuchi

Nagaoka University of Technology
1603-1 Kamitomioka, Nagaoka 940-2188, JAPAN
tnoguchi@vos.nagaokaut.ac.jp

Abstract – This paper describes a direct-power-controlled current-source PWM rectifier, and presents operation characteristics by using a 2-kW experimental setup. The key of the proposed strategy is a direct selection of switching modes on the basis of a relay control technique of instantaneous active and reactive power, using an optimum switching table. The main feature of the direct power control is high-speed response of the power control; hence inductance of the DC reactor can be reduced. Feasibility of the strategy is verified through experimental tests, using the prototype. Experimental results demonstrate that the inductance of the DC reactor can be reduced down to 0.7 mH in the prototype, achieving the 92.5-% maximum efficiency, 99.9-% maximum total input power factor, and 3.1-% total harmonic distortion of the input current. Furthermore, operation characteristics are examined under unbalanced power source condition.

I. INTRODUCTION

An AC/DC power converter is required to convert electric power from AC to DC, to obtain a stable voltage fed to a load, to improve input power factor, and to suppress harmonic currents at the same time. In order to achieve this goal, a PWM rectifier is widely used in variety of industry applications, which can be classified to a current-source PWM rectifier and a voltage-source PWM rectifier. The latter is a dual circuit of the former, and is more popular than the former.

The authors have investigated a direct power control technique of both types of the rectifiers, which allows high-speed response of the active and the reactive power control. The key feature of this technique is as follows:

- 1) No need to implement current minor loops;
- 2) No need for rotational coordinate transformation; and
- 3) Relay (bang-bang) algorithm based direct active and reactive power control.

This paper verified experimental operation characteristics of the direct power control based current-source PWM rectifier with a miniaturized DC reactor. In addition, operation performance under an unbalanced three-phase power source is discussed in the paper, which shows feasibility of the proposed strategy.

II. SYSTEM CONFIGURATION AND CONTROL ALGORITHM

A. System Configuration

Fig. 1 depicts a system configuration of the direct power

control based current-source PWM rectifier, where the instantaneous active power P and the instantaneous reactive power Q are directly controlled in a manner of relay control or bang-bang control.

In the system, power-source voltages v_u, v_v, v_w and line currents i_u, i_v, i_w are detected, using transformers and Hall-effect current transducers. These detected three-phase quantities are transformed to two-phase quantities according to (1) and (2).

$$\begin{bmatrix} v_\alpha \\ v_\beta \end{bmatrix} = \sqrt{\frac{2}{3}} \begin{bmatrix} 1 & -1/2 & -1/2 \\ 0 & \sqrt{3}/2 & -\sqrt{3}/2 \end{bmatrix} \begin{bmatrix} v_u \\ v_v \\ v_w \end{bmatrix}, \text{ and} \quad (1)$$

$$\begin{bmatrix} i_\alpha \\ i_\beta \end{bmatrix} = \sqrt{\frac{2}{3}} \begin{bmatrix} 1 & -1/2 & -1/2 \\ 0 & \sqrt{3}/2 & -\sqrt{3}/2 \end{bmatrix} \begin{bmatrix} i_u \\ i_v \\ i_w \end{bmatrix}. \quad (2)$$

The instantaneous active power P and the instantaneous reactive power Q are calculated from the results of the above transformations as follows:

$$\begin{bmatrix} P \\ Q \end{bmatrix} = \begin{bmatrix} v_\alpha & v_\beta \\ v_\beta & -v_\alpha \end{bmatrix} \begin{bmatrix} i_\alpha \\ i_\beta \end{bmatrix}. \quad (3)$$

On the other hand, the instantaneous active power command P^* is provided from a DC bus current control block, while the instantaneous reactive power command Q^* is given from outside of the system as shown in Fig. 1. If a unity total power factor operation is desired, zero command value of Q^* is given to the system, which is the most common operating condition of a grid-connected rectifier. Control errors $\Delta P = P^* - P$ and $\Delta Q = Q^* - Q$ are used to generate quantized signals S_p and S_q with hysteresis comparators. As described later on, a dither signal, which is a high-frequency triangular waveform with as minute amplitude as hysteresis bandwidth, is superposed onto the control errors to improve the operation performances. Furthermore, a phase angle of the power-source voltage vector is also quantized to 6 sectors Θ_n as shown in Fig. 2, where α -axis and β -axis denote real and imaginary parts of the vector, respectively. The quantized sectors Θ_n is mathematically expressed as

$$\frac{\pi}{6}(2n-3) \leq \Theta_n < \frac{\pi}{6}(2n-1) \quad \because n=1, 2, \dots, 6. \quad (4)$$

By using the quantized signals S_p, S_q and Θ_n , an appropriate

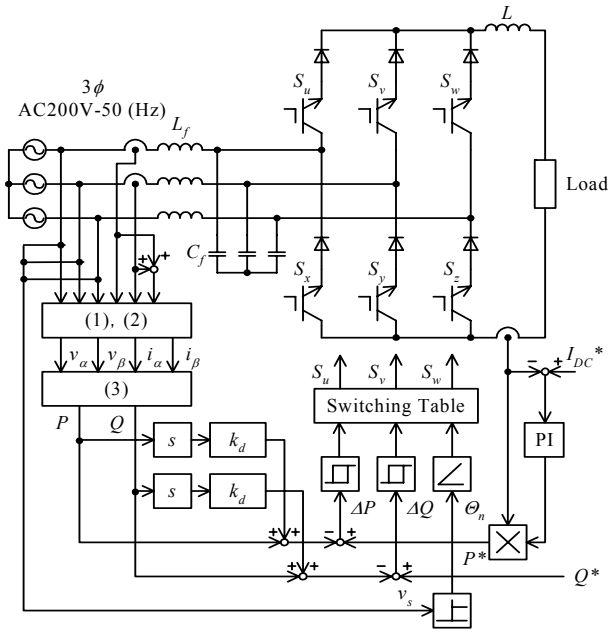


Fig. 1. System configuration of direct-power-controlled current-source PWM rectifier.

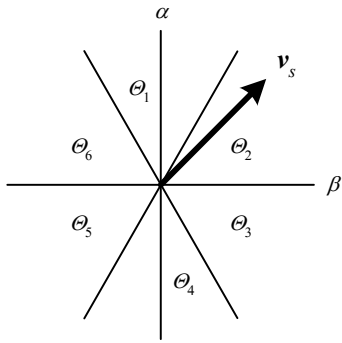


Fig. 2. Quantized phase of power-source voltage vector.

switching state of the PWM rectifier is uniquely determined to restrict the control errors ΔP and ΔQ within the hysteresis bandwidth. In other words, ascent or descent of the instantaneous power is controlled to make the actual power follow its command value within a minute tolerance. If each of S_p and S_q in a certain θ_n is "1", one of the switching states to increase the power is selected, and vice versa in the case that S_p and S_q are "0". In order to achieve this relay control operation, an optimum switching state table is employed to select unique appropriate switching state of the PWM rectifier, according to the quantized signals S_p , S_q and θ_n . Fig. 3 depicts the optimum switching state table, which generates ON or OFF control signals for each switching semiconductor device in the PWM rectifier. In the table, a switching state "P" indicates that high side devices are turned on and that low side devices are turned off, and "N" indicates vice versa. Another switching state "O" corresponds to a state that both of the high and the low side devices are simultaneously turned off. Moreover, the other switching state "S" means short circuit situation by turning on the high- and the low-side devices in one of the three legs at the same time.

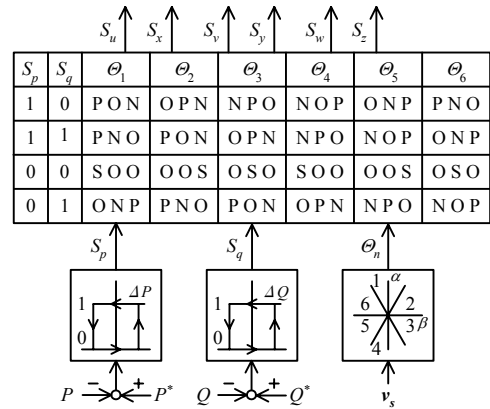


Fig. 3. Optimum switching state table and comparators for quantization.

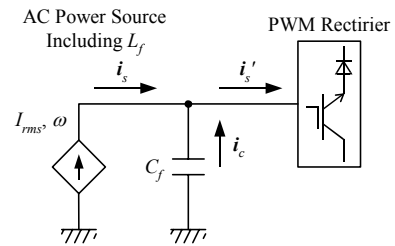


Fig. 4. Current-source PWM rectifier model.

B. Switching State Table

Since the proposed DPC system is in principle based on a relay control technique, it is significant to investigate relationship between the switching state of the PWM rectifier and polarities of time derivatives of the active and reactive power dP/dt and dQ/dt . According to the time derivatives dP/dt and dQ/dt mathematically solved in terms of the switching state of the PWM rectifier, one of the switching states of the PWM rectifier must uniquely be determined to restrict the control errors ΔP and ΔQ within the hysteresis bandwidth. In the following discussion, therefore, the time derivatives dP/dt and dQ/dt in an exceedingly short-time duration, which corresponds to a moment of switching operation in the PWM rectifier, are theoretically investigated.

Fig. 4 illustrates a grid-connected PWM rectifier model, where the power source including an inductance L_f of the input LC filter is regarded as a current source. From this model, the following circuit equation is given:

$$i_s + i_c = i_s + C_f \frac{dv_c}{dt} = i'_s. \quad (5)$$

In the above equation, a current vector of the PWM rectifier i'_s is a function of the switching state as indicated in (6), where I_{DC} is an output DC bus current.

$$i'_s = \sqrt{\frac{2}{3}} I_{DC} \left(S_u + S_v e^{j\frac{2\pi}{3}} + S_w e^{j\frac{4\pi}{3}} \right). \quad (6)$$

Each of S_u , S_v , and S_w in (6) takes one of the three values "1", "-1" and "0", which corresponds to the switching state

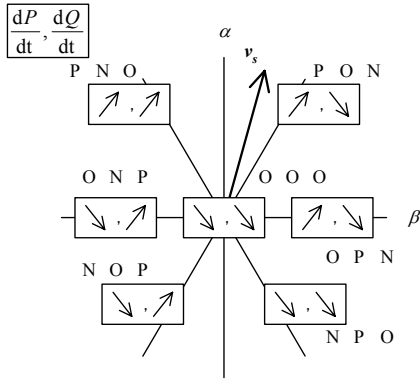


Fig. 5. Symbolized time derivatives of instantaneous active and reactive power in case of sector θ_1 .

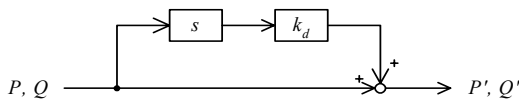


Fig. 6. Resonance suppression block.

“P”, “N”, and “O or S”, respectively. On the other hand, the power source current vector \mathbf{i}_s is defined by the following equation:

$$\mathbf{i}_s = i_\alpha + j i_\beta = \sqrt{\frac{2}{3}} \left(i_u + i_v e^{j\frac{2\pi}{3}} + i_w e^{j\frac{4\pi}{3}} \right), \quad (7)$$

$$\begin{aligned} i_u &= \sqrt{2} I_{rms} \cos \omega t \\ \therefore i_v &= \sqrt{2} I_{rms} \cos(\omega t - 2\pi/3) \\ i_w &= \sqrt{2} I_{rms} \cos(\omega t - 4\pi/3) \end{aligned} \quad (8)$$

Substituting (8) into (7), The power source current vector \mathbf{i}_s can be expressed as a rotating vector with an amplitude of $\sqrt{3} I_{rms}$ and a frequency of ω .

$$\mathbf{i}_s = \sqrt{3} I_{rms} e^{j\omega t}. \quad (9)$$

As assumed early in this discussion, since a variation of \mathbf{i}_s is negligibly small due to the input filter inductance L_f in as short-time duration as a PWM pulse period, the filter capacitance voltage v_c can nearly be regarded as the power-source voltage v_s . Therefore, the time derivatives of the active and reactive power dP/dt and dQ/dt derived from (3) can be approximated as follows:

$$\frac{dP}{dt} = \mathbf{i}_s \bullet \frac{d\mathbf{v}_s}{dt} + \frac{d\mathbf{i}_s}{dt} \bullet \mathbf{v}_s \approx \mathbf{i}_s \bullet \frac{d\mathbf{v}_c}{dt}, \text{ and} \quad (10)$$

$$\frac{dQ}{dt} = \mathbf{i}_s \times \frac{d\mathbf{v}_s}{dt} + \frac{d\mathbf{i}_s}{dt} \times \mathbf{v}_s \approx \mathbf{i}_s \times \frac{d\mathbf{v}_c}{dt}, \quad (11)$$

where \bullet and \times denote a scalar product and a vector product,

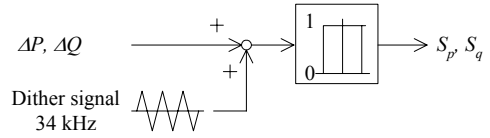


Fig. 7. Compensation by means of dithering.

TABLE I ELECTRIC PARAMETERS OF POWER CIRCUIT.

Input filter inductance L_f	2.7 mH
Input filter capacitance C_f	40 μ F
DC bus inductance L	0.7 mH
Power source voltage	200 V, 50 Hz
DC bus current command	12.5 A
Hysteresis bandwidth	100 W and 100 var
Dithering signal	150 W and 150 var, 34 KHz

respectively. Substituting (5), (6) and (9) into the above equations, dP/dt and dQ/dt are solved as follows:

$$\frac{dP}{dt} = \frac{I_{rms}}{C_f} \left[-3I_{rms} + \sqrt{2}I_{dc} \left\{ (S_u - \frac{S_v}{2} - \frac{S_w}{2}) \cos \theta + \frac{\sqrt{3}}{2} (S_v - S_w) \sin \theta \right\} \right], \text{ and} \quad (12)$$

$$\frac{dQ}{dt} = \frac{\sqrt{2}I_{rms}I_{DC}}{C_f} \left\{ -\frac{\sqrt{3}}{2} (S_s - S_t) \cos \theta + (S_r - \frac{S_s}{2} - \frac{S_t}{2}) \sin \theta \right\}, \quad (13)$$

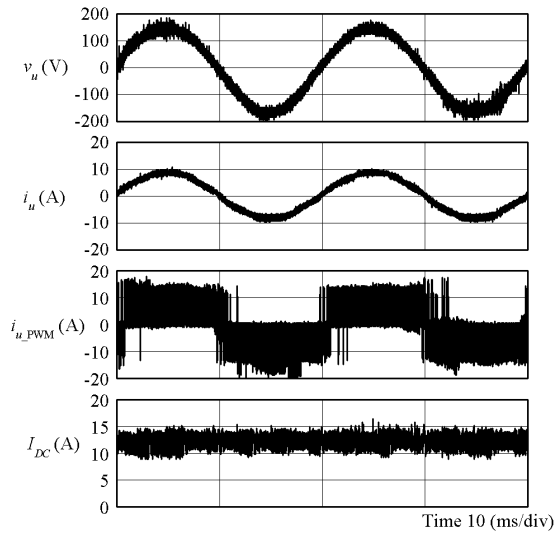
where θ is an argument of the power-source voltage vector \mathbf{v}_s shown in Fig. 2. Since both of dP/dt and dQ/dt are calculated from (12) and (13), ascent or descent of the instantaneous active and reactive power can be found in connection with the switching state of the PWM rectifier as illustrated in Fig. 5. Therefore, the contents of the optimum switching state table is theoretically determined on the basis of the above discussion.

C. LC Filter Resonance Suppression

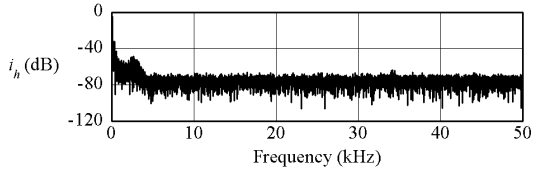
In general, a current-source PWM rectifier requires an input LC filter, which may cause current waveform distortions due to the LC resonance. Therefore, it is necessary to dump the LC resonance based oscillation with a feedback compensation technique of the instantaneous active and reactive power control loops. Fig. 6 shows a block diagram of the power feedback compensation, which is constituted by differential elements k_d . This compensation adds a dumping factor to the transfer function between the AC power source and the DC bus of the PWM rectifier.

D. Compensation by Means of Dithering

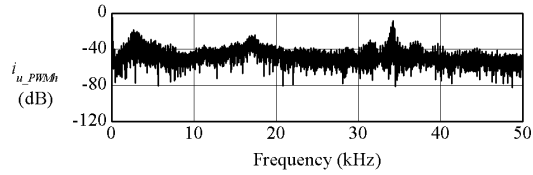
The proposed DPC strategy employs a relay control technique of the instantaneous active and reactive power to achieve ultimately high-speed response. However, switching frequency varies due to the load time constant, hysteresis



(a) Input voltage, input current, current PWM pattern, and DC bus current waveforms.



(b) FFT analysis result of input current.



(c) FFT analysis result of current PWM pattern.

Fig. 8. Waveforms and FFT analysis results in steady state.

bandwidth, and delay time of the controller, which makes the input LC filter design rather difficult. This drawback of the relay-control based system can be overcome with a compensation technique, which is called “dithering.”

Fig. 7 depicts a block diagram of the compensator by means of dithering. As shown in the figure, a high-frequency triangular signal with minute amplitude is superposed onto the control errors ΔP and ΔQ . Its amplitude is as minute as the hysteresis bandwidth of the power control loops, so the dithering technique effectively makes switching frequency almost constant in the steady state without sacrificing the inherent high-speed response in the transient.

III. EXPERIMENTAL RESULTS AND PERFORMANCE EVALUATION

A. Operation Waveforms in Steady State

In order to verify the feasibility of the proposed system, a 2-kW prototype was set up and various experimental tests were conducted. Electric parameters of the prototype power circuit are listed in TABLE I. It should be noted that the

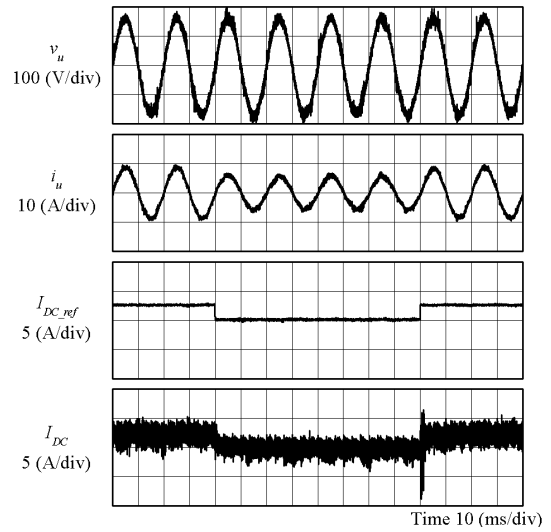


Fig. 9. DC bus current step response.

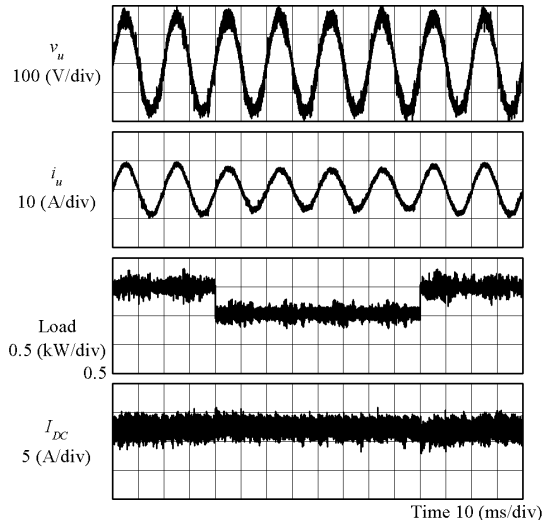


Fig. 10. Step response to sudden load change.

inductance L of the DC reactor is as low as 0.7 mH. Fig. 8 represents several operation waveforms of the prototype in the steady state, where the DC bus current command is 12.5 A and the load is 2 kW. As can be seen in the figure, the input current from the power source is in phase with the power source voltage, and has a sinusoidal waveform similarly to the voltage waveform. The DPC based PWM rectifier makes unity total power factor operation possible as shown in the figure with neither current minor loops nor rotational coordinate transformation that requires a trigonometric calculation. Furthermore, it can be seen that the DC bus current is stably regulated regardless of the small DC reactor. The FFT analysis result of the input current indicates that no conspicuous harmonic components are observed and that the frequency spectrum widely spreads over the measured range, which proves low harmonic distortion in the input current waveform. On the other hand, the current PWM waveform of the rectifier has a remarkable spectrum at 34 kHz, which is caused by the superposed triangular signal for dithering. This

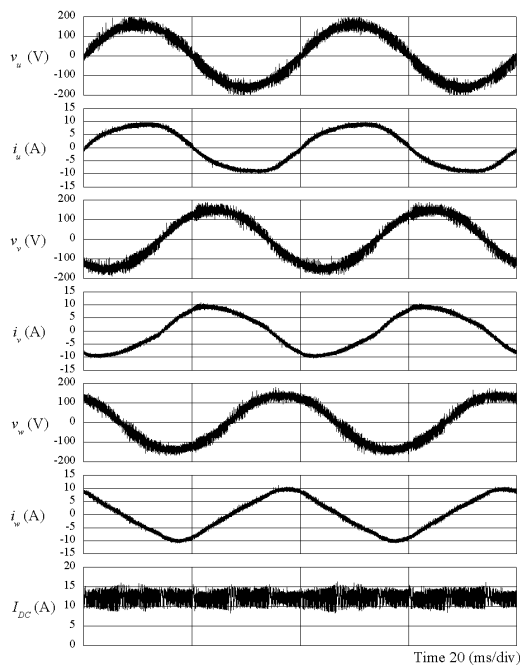


Fig. 11. Waveforms under unbalanced power source condition.

characteristic is quite similar to that of the conventional sub-harmonic modulation technique. However, dithering does not affect the transient response of the power control because the superposed triangular signal merely has as minute amplitude as the hysteresis bandwidth and power control loops have no linear regulators such as PI elements.

Fig. 9 shows a transient response when the DC bus current command is changed stepwise between 10.5 and 12.5 A. As can be seen here, the response time is approximately 2 ms and excellent transient waveforms are observed without an overshoot.

Fig. 10 is another transient response that shows waveforms in a load step change between 1.5 and 2 kW. The DC bus current is kept almost constant at the commanded value even though the sudden load change is applied.

B. Operation Characteristics under Unbalanced Power Source Condition

Assuming an unbalanced power source condition, operation characteristics of the proposed system were experimentally examined. Even in this occasion, a small reactor of 0.7 mH was used to smooth the DC bus current. The unbalanced power source voltages were $v_{uv} = 200$ V, $v_{vw} = 200$ V, $v_{wu} = 173$ V, while other test conditions were exactly same as those of TABLE I. Fig. 11 shows operation waveforms of the PWM rectifier when the load is 2 kW and the FFT analysis results of the input currents are indicated in Fig. 12. As can be seen in Fig. 11, the input current waveforms are distorted, but the DC bus current is well regulated at a commanded value without low-frequency large ripples. As described earlier in this paper, the DPC based PWM rectifier directly regulates the instantaneous power by selecting unique and the most appropriate one of possible switching states at every moment. Therefore, the DPC system carries out to transfer more active

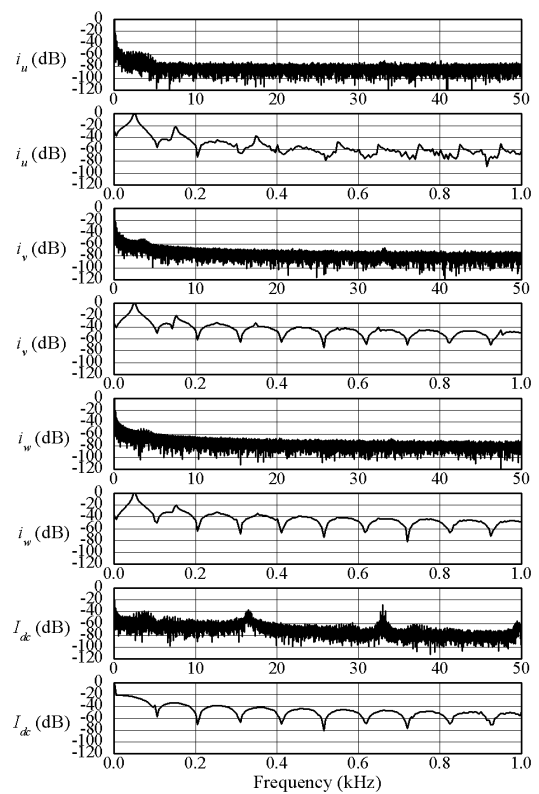


Fig. 12. FFT analysis results of input current under unbalance power source condition.

power from AC power source to the DC bus when the DC bus power goes down, and vice versa. In addition, the input current is distorted due to the third harmonics included, which is reluctantly necessary to cancel out the second harmonics caused by the unbalanced power source voltages. However, the DC bus current is smoothly maintained at a constant commanded value regardless of the small DC reactor, which is the most significant feature of the DPC system.

Fig. 13 and Fig. 14 show total efficiency and total input power factor of the DPC based prototype, respectively. Total harmonic distortion is depicted in Fig. 15 to evaluate quality of the input current waveform. These experimental data were acquired in two cases, i.e., a balanced power source condition and an unbalanced one. When the power source voltages are balanced, the maximum total efficiency of the system is 92.5 %, the maximum total input power factor is 99.9 %, and the total harmonic distortion of the input current is 3.1 % at 2-kW load. On the other hand, in the case of unbalanced power source, the maximum total efficiency and the maximum total input power factor are 92.4 % and 99.6 %, respectively. The total harmonic distortion of the input current was different among phase to phase, i.e., 7.7 % for the phase u, 7.4 % for the phase v, 8.1 % for the phase w, and Fig. 15 shows an average of these data. As is found in the experimental results, almost same performance is achieved in terms of the total efficiency in both of the balanced and the unbalanced conditions, but the total input power factor and the total harmonic distortion become worse as the load is reduced under unbalanced condition.

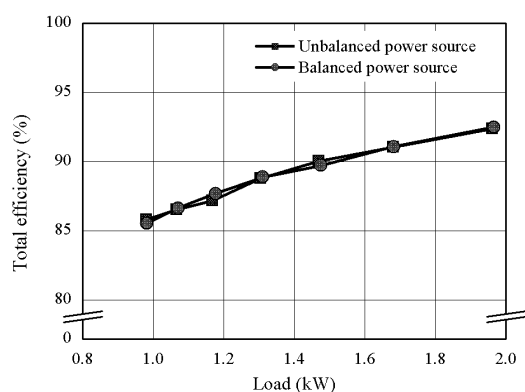


Fig. 13. Characteristics of total efficiency.

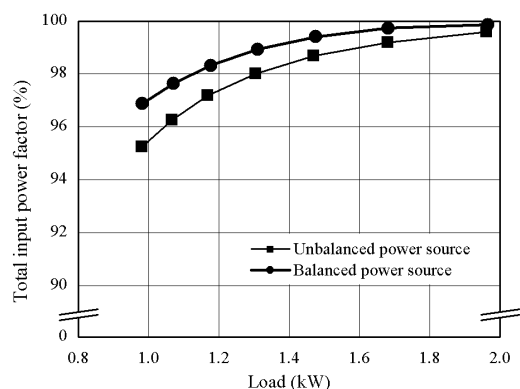


Fig. 14. Characteristics of total input power factor.

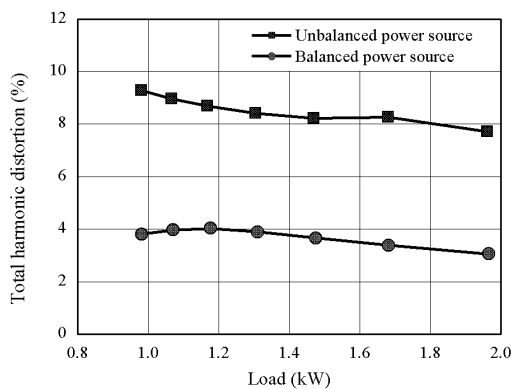


Fig. 15. Characteristics of total harmonic distortion of input current.

IV. CONCLUSION

This paper proposed a novel control strategy of a current source PWM rectifier, which features direct control of the instantaneous active and reactive power. The key of this strategy is a relay (bang-bang) control of the power by means of optimum selection of the switching state of the PWM rectifier. Owing to the relay control algorithm, the ultimately high-speed response of the instantaneous power control is achieved with neither current minor loops nor complicated signal processing such as a rotational coordinate transformation. In the theoretical analysis of the proposed

strategy, a relationship between the switching state of the PWM rectifier and the instantaneous active and reactive power was clarified, which was essential to select uniquely the most appropriate switching state with a switching table. In addition, feasibility of the system was examined through various experimental tests, using a 2-kW prototype. From the experimental results in the steady state, it was found that the proposed strategy makes it possible to obtain unity total input power factor by setting the reactive power command at zero. In other words, the input current waveform was automatically controlled to be sinusoidal and to be in phase with the power source voltage with neither current minor loops nor trigonometric calculations. Also, the ultimately high-speed response of the power control allows minimization of the DC bus reactor and a few-ms time response to the DC bus current command and to the disturbance load change.

Furthermore, operation characteristics under an unbalanced power source condition were experimentally investigated with a small DC reactor of 0.7 mH. The proposed direct power control technique is capable to regulate the DC bus current sufficiently stable without low-frequency large ripples although the power source voltages are unbalanced. This is the significantly unique feature of the proposed direct power control strategy.

V. REFERENCES

- [1] T. Ohnishi, "Three-Phase PWM Converter/Inverter by Means of Instantaneous Active and Reactive Power Control," *IEEE IECON Proc.*, vol. 1, 1991, p.p. 819-824.
- [2] T. Noguchi, H. Tomiki, S. Kondo, and I. Takahashi, "Direct Power Control of PWM Converter Without Power-Source Voltage Sensors," *IEEE Trans. Ind. App.*, vol. 34, no. 3, 1998, p.p. 473-479.
- [3] M. Malinowski, M. Jesinski, and M. P. Kazmierkowski, "Simple Direct Power Control of Three-Phase PWM Rectifier Using Space-Vector Modulation (DPC-SVM)," *IEEE Trans. Ind. App.*, vol.51, no.2, 2004, p.p.447-454.
- [4] T. Ohnishi, and Y. Minamoto, "Three Phase Current Fed Type PWM Converter by Direct control of Instantaneous Current Vector", *IEEJ Trans. Ind. App.*, vol. 115-D, no. 8, 1995, p.p.948-990.
- [5] K. Toyama, O. Mizuno, T. Takeshita, and N. Matsui, "Suppression for Transient Oscillation of Input Voltage and Current-Source Three-Phase AC/DC PWM Converter", *IEEJ Trans. Ind. App.*, vol. 117-D, no. 4, 1997, p.p.420-426.
- [6] Y. Sato, T. Kataoka, "An Investigation of Waveform Distortion and Transient Oscillation of Input Current in Current Type PWM Rectifiers", *IEEJ Trans. Ind. App.*, vol. 114-D, no. 12, 1994, p.p.1249-1256.
- [7] S. Nakatomi, A. Sato, and T. Noguchi, "Operation Characteristics of Direct-Power-Controlled Current-Source PWM Converter", *IEEJ Ind. App. Soc. Conf Proc.*, vol.1, 2004, p.p.127-128.